energies

MDPI

Article

A Fault-Tolerant Strategy for Three-Level Flying-Capacitor DC/DC Converter in Spacecraft Power System †

Haijin Li [1,*], Yu Gu [2], Xiaofeng Zhang [1], Zhigang Liu [1], Longlong Zhang [3] and Yi Zeng [1]

[1] Beijing Institute of Spacecraft System Engineering, Beijing 100094, China
[2] School of Mechanical Engineering and Automation, Harbin Institute of Technology (Shenzhen), Shenzhen 518055, China
[3] Department of Electrical Engineering, China University of Petroleum (East China), Qingdao 266580, China
* Correspondence: haijinli@126.com
† This paper is an extended version of our paper published in 2022 IEEE International Power Electronics and Application Conference and Exposition (PEAC), Guangzhou, China, 4–7 November 2022; pp. 1620–1625.

Abstract: With the development of space exploration, high-power and high-voltage power systems are essential for future spacecraft applications. Because of the effects of space radiation such as single event burnout (SEB), the rated voltage of power devices in converters for a spacecraft power system is limited to a level much lower than that for traditional ground applications. Thus, multi-level DC/DC converters are good choices for high-voltage applications in spacecraft. In this paper, a fault-tolerant strategy is proposed for a three-level flying capacitor DC/DC converter to increase the reliability with minimal cost. There is no extra hardware needed for the proposed strategy; the fault tolerance of the converter is only achieved by changing the software control strategy. A stage analysis of the proposed strategy is provided in detail for different fault locations and ratios between the input and output voltage. Finally, a simulation model and prototype are built to verify the effectiveness of the proposed strategy.

Keywords: fault-tolerant strategy; high voltage; three level; flying capacitor; DC/DC converter; spacecraft power system

Citation: Li, H.; Gu, Y.; Zhang, X.; Liu, Z.; Zhang, L.; Zeng, Y. A Fault-Tolerant Strategy for Three-Level Flying-Capacitor DC/DC Converter in Spacecraft Power System. *Energies* **2023**, *16*, 556. https://doi.org/10.3390/en16010556

Academic Editor: Md Rasheduzzaman

Received: 21 November 2022
Revised: 24 December 2022
Accepted: 26 December 2022
Published: 3 January 2023

1. Introduction

The architecture of a high-power spacecraft distributed power system is shown in Figure 1. The spacecraft power system is a typical DC power system [1,2]. It consists of solar arrays, batteries, a fuel cell, flying wheel, power converters, etc. The solar arrays provide the power for the load and charge the battery during the sunlight period of the orbit. Storages such as batteries provide the power for the load during the eclipse period of the orbit. The power converters are used to regulate the DC bus voltage and control the battery charging and discharging. With the development of space exploration, the power capacity of spacecraft has become larger and larger, and the voltage level of the spacecraft power system has become higher and higher. Currently, high voltage and high power are the trends and necessary factors for a spacecraft power system to meet the requirements of future spacecraft, such as high-power SAR satellites, electric propulsion spacecraft, deep space spacecraft, space stations, and space solar energy power stations, etc. [3] The power ratings of these spacecraft will need to be larger than 100 kW, and the voltage level will need to be higher than 1000 V. However, the current power converters cannot meet the requirements of this high-voltage application. The characteristics of the power device in space are obviously different from that on the ground. Due to space radiation effects such as single event burnout, the high-voltage power device is the main limitation for spacecraft power converters. Currently, the available voltage of power devices such as power MOSFETs for spacecraft power converters is lower than 500 V. However, the requirement of the output voltage of converters is much higher than 500 V for future space

applications. In order to solve the mismatch between future high-voltage applications and the available low-voltage power devices, the multi-level DC/DC converter is a better solution for these high-voltage applications with the voltage limitation of the power devices. Even though they are not used in traditional spacecraft power systems in which the highest DC bus voltage is 100 V, these converters are widely used in ground high-voltage applications. The voltage stress of the power devices in a multi-level DC/DC converter can clearly be reduced [4–10]. For multi-level DC/DC converters, the number of power devices is relatively larger than the traditional two-level converter. Each failure of the power device may cause the output interruption of the converter, so the reliability of the multi-level DC/DC converter is relatively low without a fault-tolerant strategy [11–16]. In addition, the reliability of the converter is very important for the spacecraft. The failure of the converter will result in huge losses, especially for an unmanned spacecraft. Thus, the fault-tolerant strategy is very important for the multi-level converter in a spacecraft power system. Fault-tolerant schemes of multi-level DC/DC converters have been proposed by researchers [14–20]. The redundant subsystem, units, circuits, or devices have been added to multi-level converters to improve their reliability [14,15,17,18]. The fuse is a common component that is used to isolate the short-circuit fault parts of the converter. The main disadvantage of the fuses is that the blowing time of a fuse is difficult to control. Moreover, the use of a fuse will increase the parasitic inductance of the commutation loops of the converter, and larger parasitic inductance causes a higher voltage stress, which reduces the reliability of power devices [19,20]. Additional hardware is needed for these former methods. However, the additional hardware increases the mass of the converter, which results in an obviously higher cost of the launch. For space application, the limitation of the mass of converters is extremely strict. A three-level flying capacitor DC/DC converter is the typical multi-level DC/DC converter. A fault-tolerant control strategy for three-level flying capacitor DC/DC converters is proposed in this paper. The reliability of the three-level DC/DC converter is improved with minimal cost. The fault tolerance of the converter is achieved by only changing the software strategy, and no extra hardware is needed. The concept of the fault-tolerant strategy can also be applied in other multi-level converters.

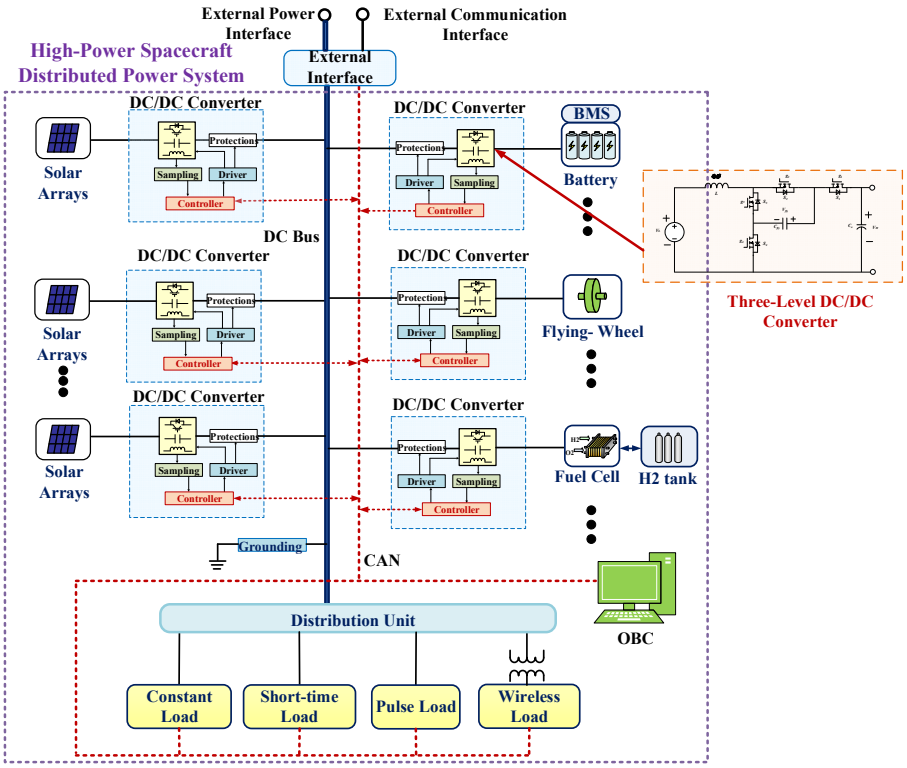

Figure 1. Typical high-power spacecraft distributed power system with DC/DC converters.

In Section 2, the control scheme of the fault-tolerant strategy for a three-level flying capacitor DC/DC converter is introduced. In Section 3, the stage analysis of the converter under short-circuit fault conditions is given in detail. In Section 4, the proposed strategy under different conditions is verified by experiments and simulations. Finally, the conclusions are summarized.

2. Control Scheme of Fault-Tolerant Strategy for Three-Level Flying Capacitor DC/DC Converter

In order to achieve the fault-tolerant operation of the three-level flying capacitor DC/DC converter after a short-circuit fault of the power devices, a seamless transfer control from three-level mode to two-level mode is designed. Before the fault, the converter operates in three-level mode, and after the fault, the converter operates in two-level mode. The control scheme of the proposed fault-tolerant strategy for a three-level flying capacitor DC/DC converter is shown in Figure 2.

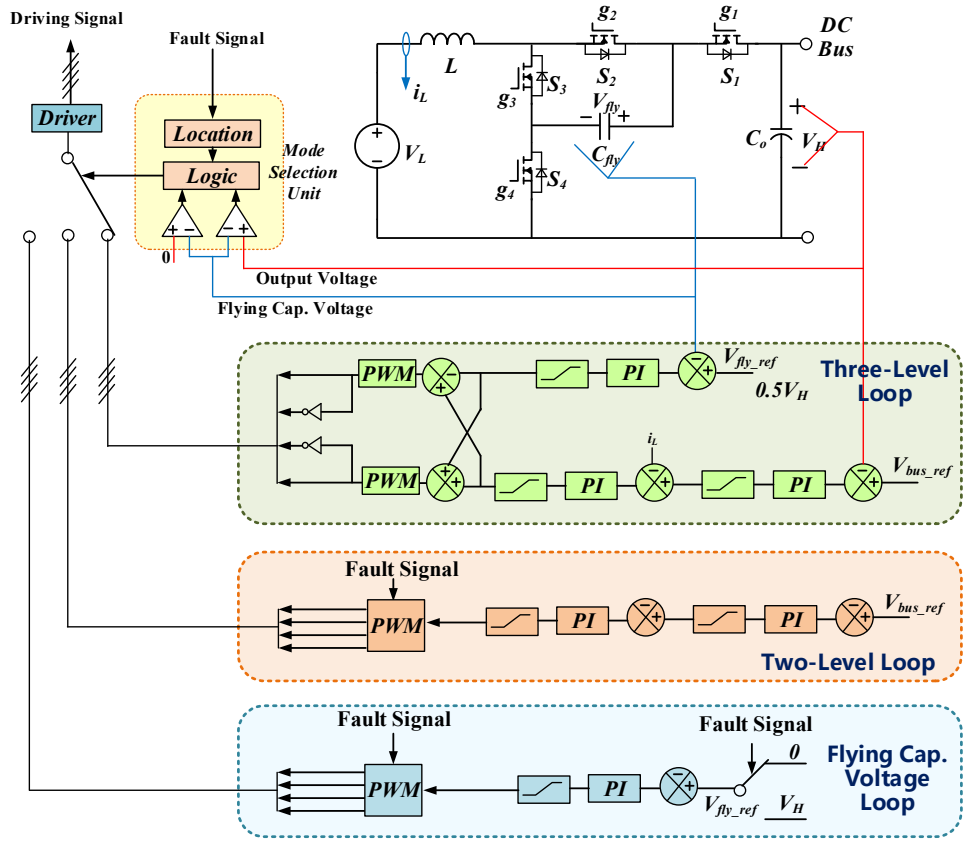

Figure 2. Control scheme of the fault-tolerant strategy for flying capacitor DC/DC converter.

The fault-tolerant strategy consists of three loops, including a three-level voltage regulation loop, a flying capacitor voltage loop, and a two-level voltage regulation loop. When the power devices of the converter are normal, the output voltage and flying capacitor voltage are regulated by a three-level voltage regulation loop. Output voltage and flying capacitor voltage are two control targets for the three-level voltage regulation loop. The reference of flying capacitor voltage is half of the reference of the output voltage of the converter. When a short-circuit fault of the power device occurs, the converter is regulated by the flying capacitor voltage loop after the short-circuit fault of the power device is detected. If a short-circuit fault of inner switch S_2 or S_3 occurs, the voltage reference of the flying capacitor changes from half of the output voltage to zero. The normal inner power devices are opened immediately, and the driver signals of the normal inner switches are set as low. If a short-circuit fault of outer switch S_1 or S_4 occurs, the reference of the

flying capacitor voltage changes from half of the output voltage to the output voltage, and the driver signals of the normal outer switches are set as high. When the voltage of the flying capacitor reaches the reference value, the converter changes its mode to the two-level mode. If the inner switch is at fault, the driver of the other inner switch is set as high in the two-level mode. The driver signals of the two outer switches operate in the complementary state. If the outer switch is at fault, the driver of the other outer switch is set as high. The driver signals of the two inner switches operate in the complementary state.

3. Analysis of Operation Modes for the Converter under Short-Circuit Fault Conditions

According to the analysis of the flying capacitor three-level DC/DC converter, the operation stages of the converter are different between the situation in which the ratio of the input and output voltage is smaller than 0.5 ($V_L < 0.5\ V_H$) and the situation in which the ratio is larger than 0.5 ($V_L > 0.5\ V_H$).

The diagram in Figure 3 shows the key quantity for the situation in which the short-circuit fault occurs in switch S_3 when the ratio of the input and output voltage is smaller than 0.5 ($V_L < 0.5\ V_H$). When the short-circuit fault of switch S_3 is detected by the detection circuit, the converter is regulated from the three-level mode to the flying capacitor voltage control mode. The reference of the flying capacitor voltage decreases from half of the output voltage V_H to zero. The voltage of the flying capacitor is changed by the flying capacitor voltage loop from half of the output voltage to zero during this stage. After the voltage of the flying capacitor is detected to have reached zero, the converter finishes the flying capacitor voltage control mode and begins to operate in two-level mode.

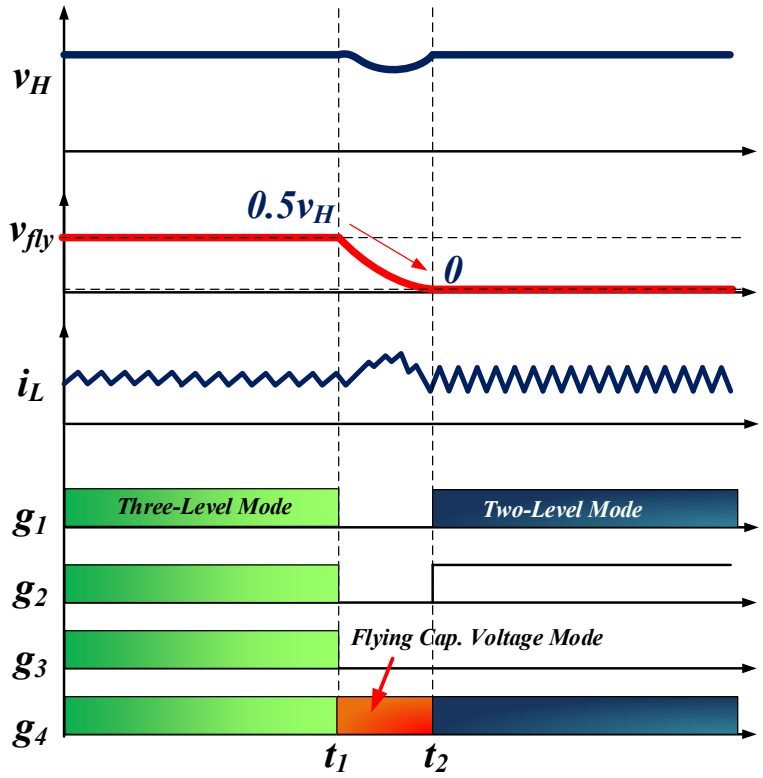

Figure 3. The diagram of the key quantity under the situation in which short-circuit fault occurs in switch S_3.

The analysis of operation stages under this fault situation is shown in Figure 4. The g_1, g_2, g_3, and g_4 are gate drivers of switches S_1, S_2, S_3, and S_4, respectively. When $V_L < 0.5\ V_H$, the duty cycle of inner switches g_3 and g_4 is larger than 0.5. The three-level mode is the pre-fault mode. The stages of the three-level mode are shown in Figure 5. There are

four stages in the three-level mode. In the three-level mode, the driver signal of g_1 and g_4 are complementary, and the driver signal of g_2 and g_3 are complementary.

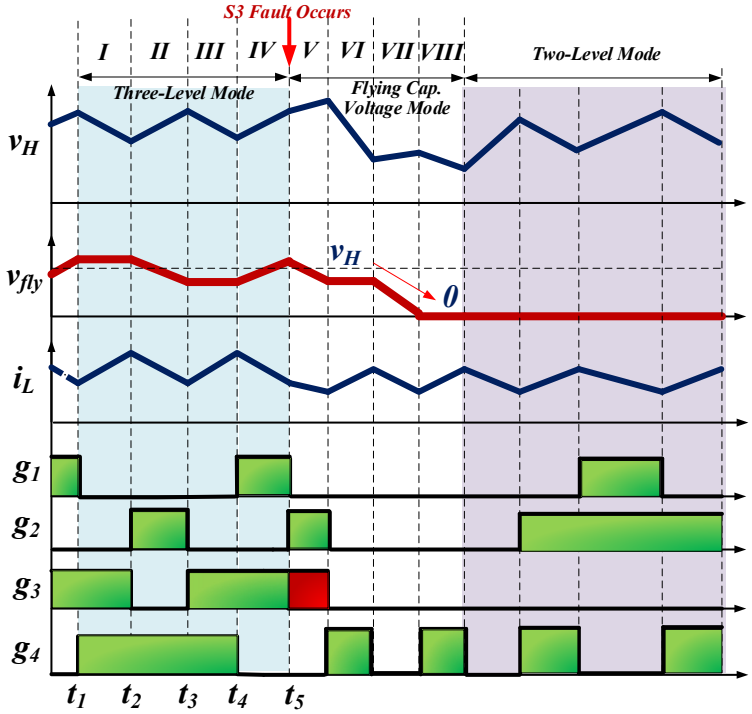

Figure 4. Stages analysis when short-circuit fault occurs in S_3 ($V_L < 0.5\ V_H$).

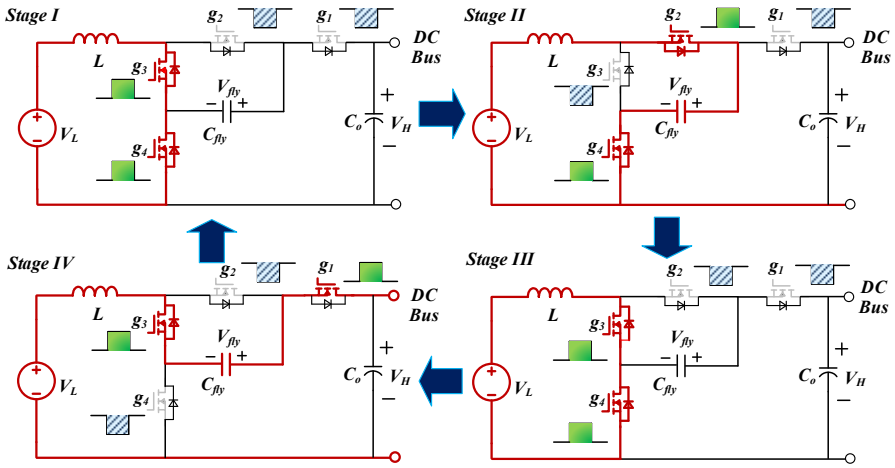

Figure 5. Stages of the three-level mode when $V_L < 0.5\ V_H$.

The stages during the flying capacitor voltage control mode are shown in Figure 6. There are also three stages after the short-circuit fault occurs. In Stage V, S_3 is short-circuited and S_2 turns on, then the flying capacitor is short-circuited. There is a large current spike occurring in S_2, so the fault is detected. After the fault is detected, the converter operates in Stage VI and VIII; in these two stages, g_4 is in the PWM state, and the values of g_1, g_2, and g_3 are 0 when the short-circuit fault occurs in S_3. Similarly, g_1 is in the PWM state, and the values of g_2, g_3, and g_4 are 0 when the short-circuit fault occurs in switch S_2. The two-level mode is the post-fault mode. In the two-level mode, the driver signal of g_1 and g_4 are complementary, and g_2 is set as 1 when the short-circuit fault occurs in switch S_3. Similarly, g_3 is set as 1 when S_2 is where the fault occurs.

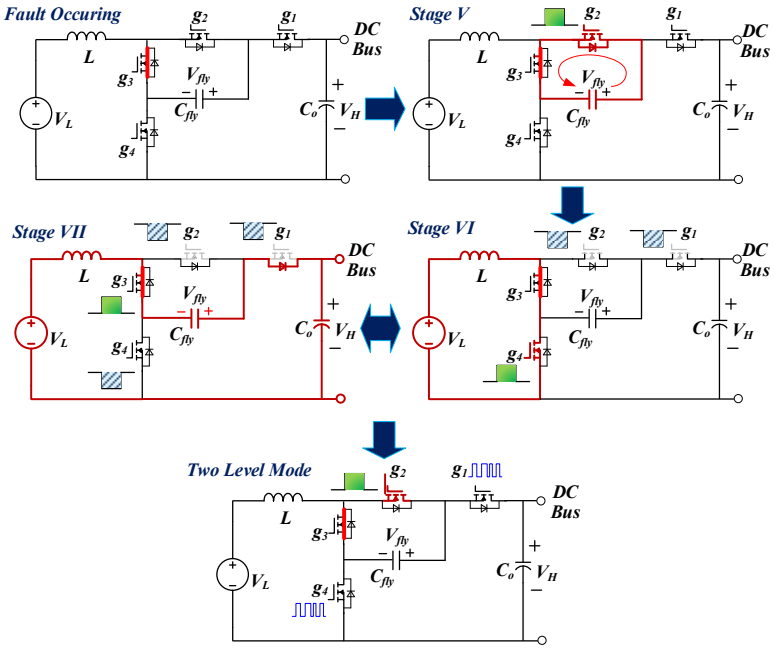

Figure 6. Stages of capacitor voltage control mode after short-circuit fault occurs in S_3.

The diagram in Figure 7 shows the key quantities under the situation in which the short-circuit fault occurs in the outer switch S_4 when V_L is lower than 0.5 V_H. Before the fault occurs, the converter operates in three-level mode. When the short-circuit fault of the switch S_4 is detected, the converter begins to operate in flying capacitor voltage control mode. The flying capacitor voltage is regulated gradually from half of the output voltage to output voltage. When the flying capacitor voltage reaches the output voltage, the converter turns to operate in two-level mode.

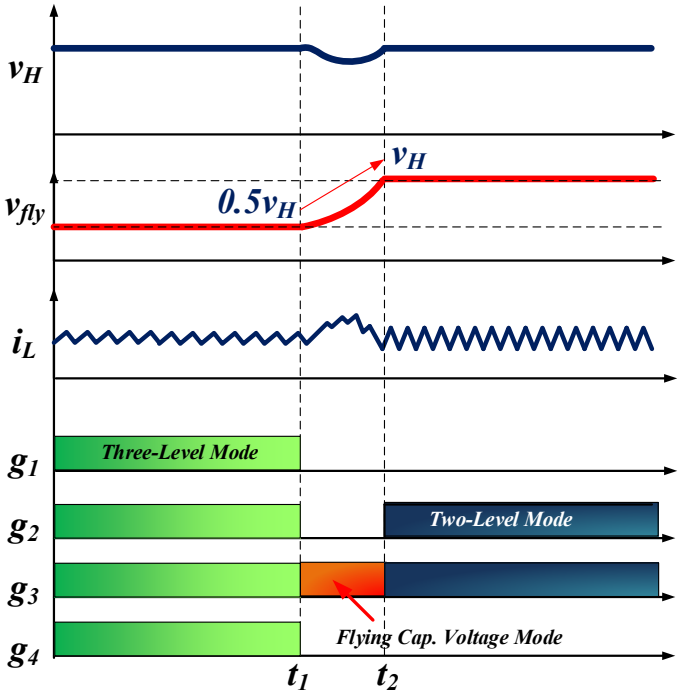

Figure 7. The diagram of the key quantity under the situation in which short-circuit fault occurs in switch S_4.

The stage analysis in this situation is shown in Figure 8. The stages of the three-level mode are the same as those in which the short-circuit fault of S_3 occurs. The stages of the flying capacitor voltage control mode after a short-circuit fault are shown in Figure 9. There are three stages after the short-circuit fault occurs in the outer switches. In Stage V of the flying capacitor voltage mode, g_4 is short-circuited and g_1 turns on; then the output capacitor is connected directly with the flying capacitor. Due to the existence of the voltage difference between the output voltage and the flying capacitor voltage, there is a current spike occurring in S_1, and the fault can be detected. After Stage V, the converter operates in Stages VI and VII. In these two stages, g_3 is in the PWM state, and g_1, g_2, and g_4 are 0 when the short-circuit fault occurs in S_4. Similarly, g_2 is in the PWM state, and g_1, g_3, and g_4 are 0 when the short-circuit fault occurs in S_1. In the two-level mode, the driver signal of g_2 and g_3 are complementary, and g_1 is set as 1 when the fault occurs in S_4. Similarly, g_4 is set as 1 when the fault occurs in S_1.

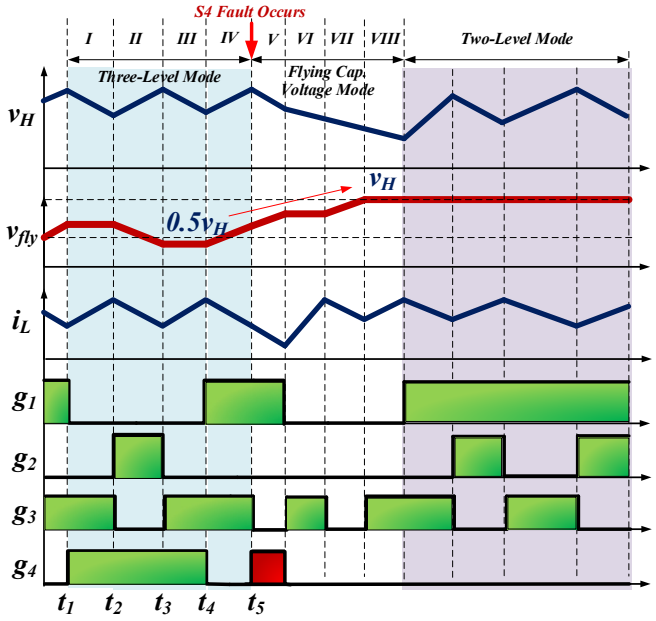

Figure 8. Stage analysis ($V_L < 0.5\ V_H$).

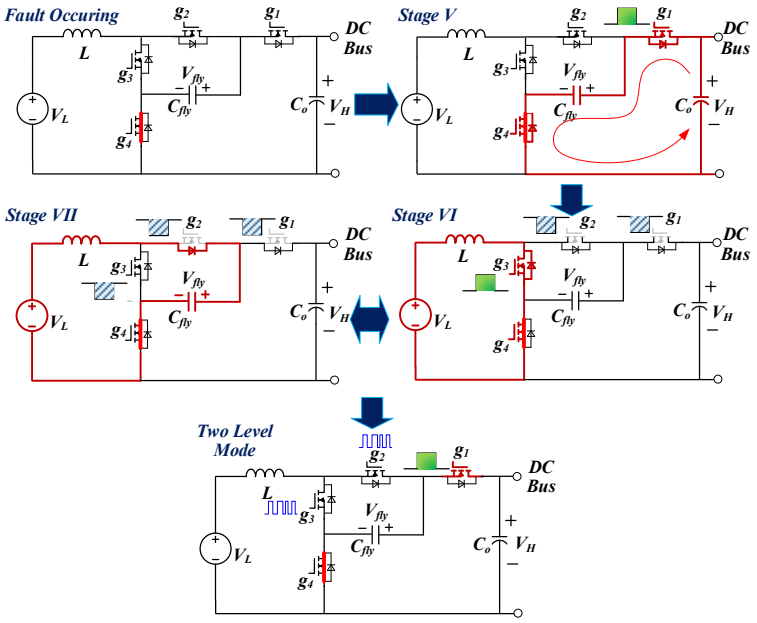

Figure 9. Stages of S_4 short-circuited.

Then the situation when V_L is higher than 0.5 V_H is analyzed in detail. The stage analysis is shown in Figure 10 for when S_3 is short-circuited in this situation. This situation is different from the situation when V_L is lower than 0.5 V_H. The duty cycle of g_3 and g_4 is less than 0.5.

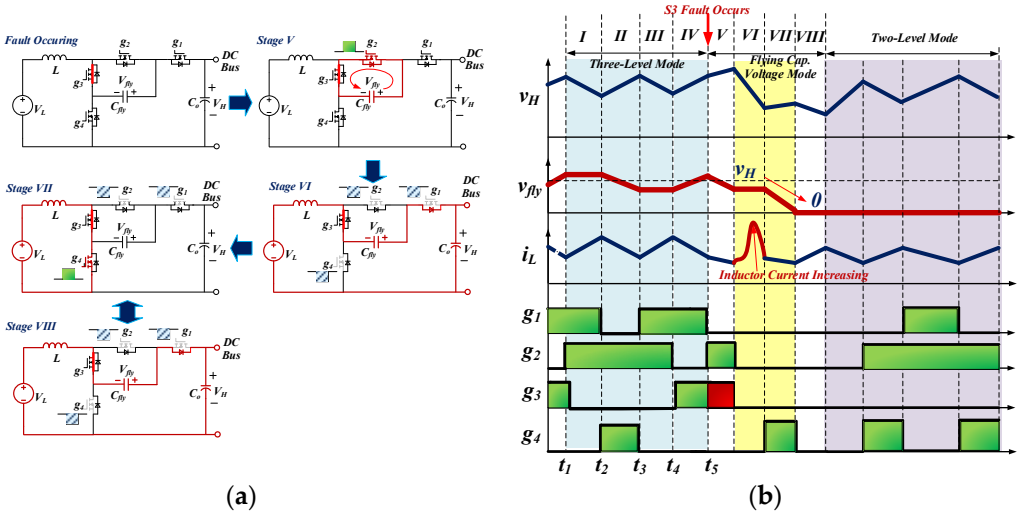

Figure 10. Short-circuit fault analysis (V_L > 0.5 V_H). (**a**) The stages when S_3 is short-circuited; (**b**) stage analysis.

When the short-circuit fault of S_3 is detected, the converter is regulated by the flying capacitor voltage control loop. Then S_4 is opened. Because V_L > 0.5 V_H and the initial value of v_{fly} is half of v_H, inequality (1) can be derived at the beginning of the fault. The voltage difference between the inductor is always positive. It should be noticed that if inequality (2) holds, the current of the inductor will continue to increase during Stage VI. When v_{fly} is lower than $(v_H - v_L)$, the converter operates in Stages VII and VIII. When the flying capacitor voltage reaches 0, the converter turns into the two-level mode, and the S_2 is closed.

$$v_L > v_H - v_{fly} \ \ (v_L > 0.5v_H, V_{fly} = 0.5v_H) \tag{1}$$

$$v_{fly} > v_H - v_L \tag{2}$$

The proper inductance value of the inductor L should be designed, and additional an over-current protection method should be considered. The flying capacitor voltage and inductor current can be calculated by (3). The current spike analysis in this situation when S_3 is short-circuited is shown in Figure 11.

$$\begin{cases} v_{fly}(\mathrm{t}) = \frac{I_L\sqrt{LC}}{C}\sin(\frac{1}{\sqrt{LC}}\mathrm{t}) + (V_{fly} - V_H + V_L)\cos(\frac{1}{\sqrt{LC}}\mathrm{t}) + (V_H - V_L) \\ i_L(\mathrm{t}) = I_L\cos(\frac{1}{\sqrt{LC}}\mathrm{t}) - \frac{(V_{fly} - V_H + V_L)C}{\sqrt{LC}}\sin(\frac{1}{\sqrt{LC}}\mathrm{t}) \end{cases} \tag{3}$$

where v_{fly} is the flying capacitor voltage, V_H is the output voltage, V_L is the input voltage, L is the inductance of the input inductor, C is the capacitance of the flying capacitor, i_L is the current value of the inductor, and I_L is the initial value of the inductor current. If the output voltage is 100 V, the input voltage is 80 V, the inductor is 1 mH, and the initial current of the inductor is 10 A, then it can be calculated that the maximum inductor current is 17.2 A. The maximum current under different levels of inductance when S_3 is short-circuited is shown in Figure 12.

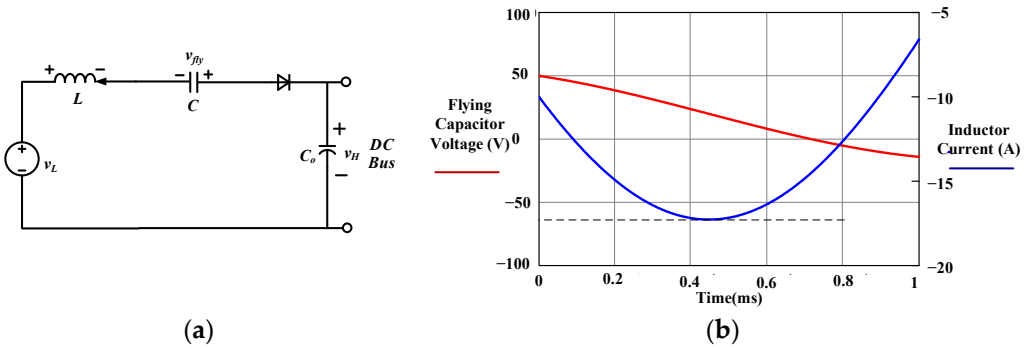

Figure 11. The analysis of the stages under S_3 fault. (**a**) Equivalent circuit; (**b**) the simulation curve (V_L 80 V, V_H 100 V, initial value of I_L-10 A).

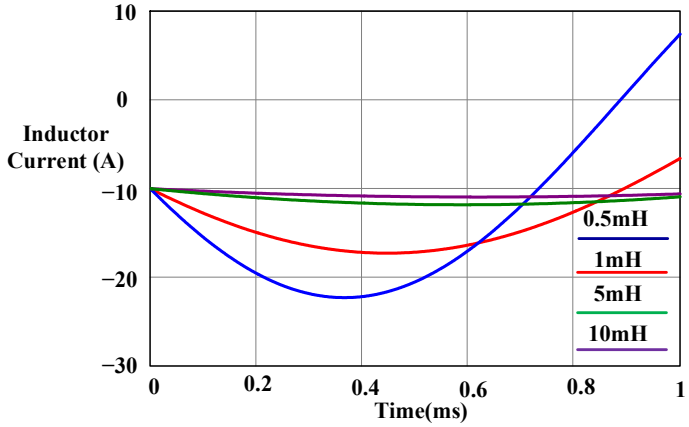

Figure 12. Maximum current under different levels of inductance when S_3 is short-circuited.

The current spike analysis when S_4 is short-circuited is shown in Figure 13. When the short-circuit fault of S_4 is detected, S_3 is turned off. Because v_L is larger than 0.5 V_H and the initial value of V_{fly} is half of V_H, inequality (4) can be derived at the beginning of the fault. The voltage difference between the inductor is always positive. It should be noticed that if inequality (5) holds, the current of the inductor will continue to increase during Stage VI. When v_{fly} is higher than 0.5 V_H, the converter operates in Stages VII and VIII.

$$v_L > v_{fly} \ \ (v_L > 0.5v_H, V_{fly} = 0.5v_H) \tag{4}$$

$$v_{fly} < 0.5v_H \tag{5}$$

When the voltage of the flying capacitor voltage reaches V_H, S_1 is turned off. The proper inductance should also be designed carefully. The flying capacitor voltage and inductor current can be calculated by (4). The current spike analysis is given in Figure 14. If we take the same parameters as the situation when S3 is faulty, the maximum inductor current is 17.2 A. The maximum current under different levels of inductance when S_4 is short-circuited is shown in Figure 15.

$$\begin{cases} v_{fly}(\mathrm{t}) = \frac{I_L\sqrt{LC}}{C}\sin(\frac{1}{\sqrt{LC}}\mathrm{t}) + (V_{fly} - V_L)\cos(\frac{1}{\sqrt{LC}}\mathrm{t}) + (V_L) \\ i_L(\mathrm{t}) = I_L\cos(\frac{1}{\sqrt{LC}}\mathrm{t}) - \frac{(V_{fly}-V_L)C}{\sqrt{LC}}\sin(\frac{1}{\sqrt{LC}}\mathrm{t}) \end{cases} \tag{6}$$

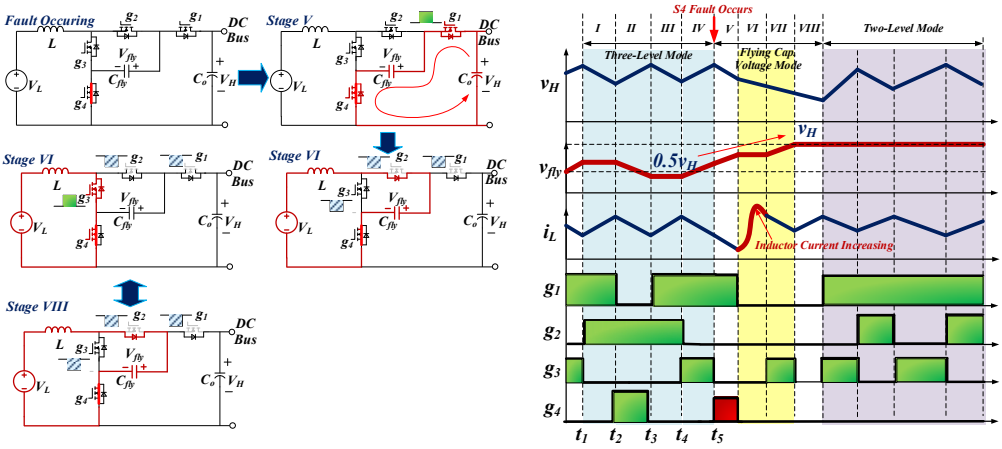

Figure 13. Short-circuit fault analysis (V_L > 0.5 V_H). (**a**) The stages when S_4 is short-circuited; (**b**) stage analysis.

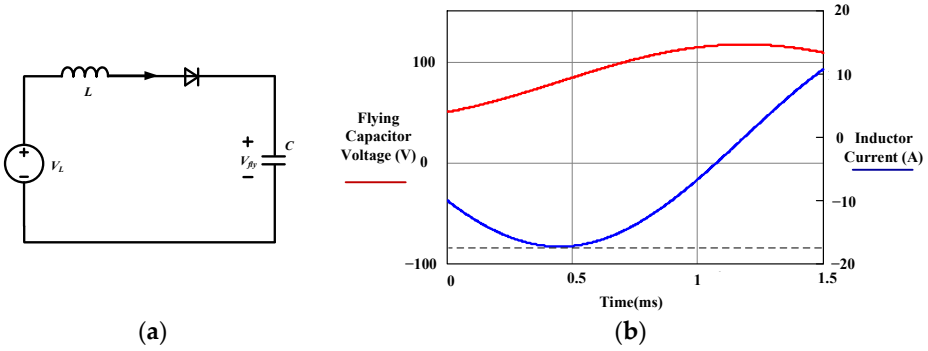

Figure 14. The analysis of the stages under S_4 fault. (**a**) Equivalent circuit; (**b**) the simulation curve (V_L 80 V, V_H 100 V, initial value of I_L 10 A).

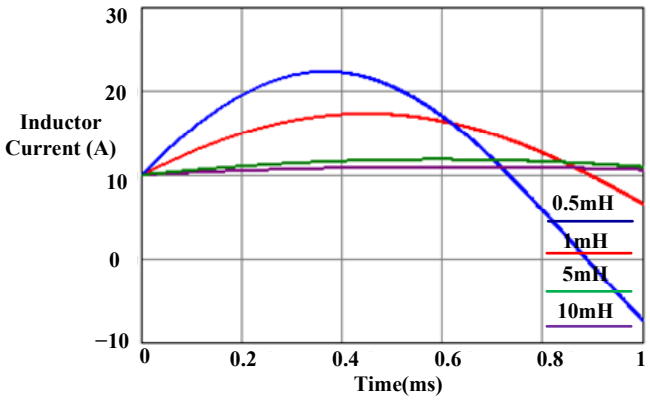

Figure 15. Maximum current under different levels of inductance when S_4 is short-circuited.

The parameters of the flying capacitor DC/DC converter can be calculated as below. According to the stage analysis of the circuit, the inductance of the input inductor is derived by (7), the capacitance of the flying capacitor is derived by (8), and the capacitance of the output capacitor is derived by (9).

$$L_{IN} = \begin{cases} \frac{(\frac{U_o}{2} - U_{IN})(1-D)}{\delta_I I_{in} \cdot f_s} & (D > 0.5) \\ \frac{(U_{IN} - \frac{U_o}{2}) \cdot D}{\delta_I I_{in} \cdot f_s} & (D < 0.5) \end{cases} \quad (7)$$

$$C_{fly} = \begin{cases} \frac{I_{IN}(1-D)}{\frac{\delta_f U_o}{2} \cdot f_s} & (D > 0.5) \\ \frac{I_{IN} D}{\frac{\delta_f U_o}{2} \cdot f_s} & (D < 0.5) \end{cases} \quad (8)$$

$$C_o = \frac{I_o}{\delta_o U_o \cdot f_s} \quad (9)$$

where the output voltage U_o is 100 V, the input voltage U_{IN} is 30~80 V, the switching frequency f_s is 10,000 Hz, the duty cycle D is 0.2~0.7, the input current I_{IN} is 33 A, the output current Io is 10 A, the ripple ratio of the input current δ_I is 0.02, the ripple ratio of the flying capacitor voltage δ_f is 0.1, and the ripple ratio of the output capacitor voltage δ_o is 0.01. Then the inductor is 0.9 mH, the flying capacitor is 200 µF, and the output capacitor is 1 mF. With the consideration of the current spike analysis after a short-circuit fault in the simulation, the inductance of the inductor is chosen as 1 mH, and the capacitances of the flying capacitor and the output capacitor are chosen as 200 µF and 1 mF, respectively.

4. Simulation and Experiment Verifications of the Fault-Tolerant Strategy

In order to verify the proposed fault-tolerant strategy, the simulation model of the flying capacitor three-level DC/DC converter based on PSIM was built. In the model, the rated power of the flying capacitor three-level converter is 1 kW. The output voltage of the converter is 100 V. The two types of input voltage are considered, including 30 V (V_L<0.5 V_H) and 80 V (V_L > 0.5 V_H). The inductance of the inductor is 1 mH. The capacitance of the flying capacitor is 200 uF, and the capacitance of the output capacitor is 1 mF. The parameters of the simulation are shown in Table 1.

Table 1. The parameters of the different simulation cases.

Item	Case I (Figure 16) Value	Case II (Figure 17) Value	Case III (Figure 18) Value	Case IV (Figure 19) Value
Input voltage	30 V	30 V	80 V	80 V
Output DC bus voltage	100 V	100 V	100 V	100 V
Input inductor	1 mH	1 mH	1 mH	1 mH
Flying capacitor	200 µF	200 µF	200 µF	200 µF
Output bus capacitor	1 mF	1 mF	1 mF	1 mF
Load power	100 W/1000 W	100 W/1000 W	100 W/1000 W	100 W/1000 W
Fault location	Inner switch S_3	Outer switch S_4	Inner switch S_3	Outer switch S_4

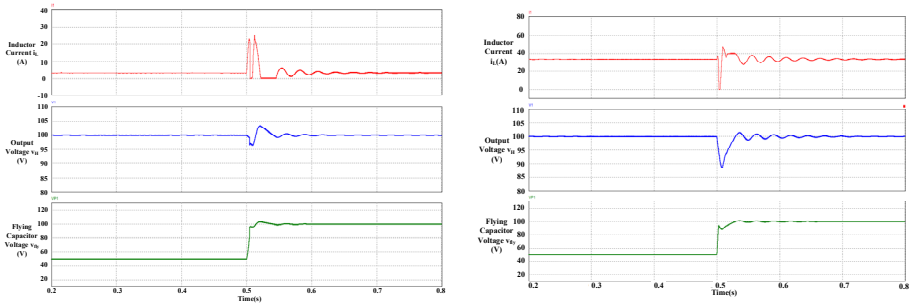

(**a**) (**b**)

Figure 16. The waveforms of S_4 short-circuit fault (V_L < 0.5 V_H). (**a**) Light load 100 W; (**b**) heavy load 1000 W.

The simulation waveforms when a short-circuit fault occurs in outer switch S_4 under two load conditions are shown in Figure 16. It can be seen that the output voltage of the converter is uninterruptible when a short-circuit fault of S_4 occurs. The mode transfer after the fault is seamless.

The simulation results when the input voltage is lower than half of the output voltage are shown in Figure 17. The waveforms when a short-circuit fault occurs in inner switch

S_3 under different load conditions are shown in Figure 17a,b. The two load conditions are 100 W for a light load and 1000 W for a heavy load. It can be seen that the output voltage of the converter is uninterruptible after the S_3 fault occurs. The spike of the current and voltage is in the normal range during the mode transition after the fault.

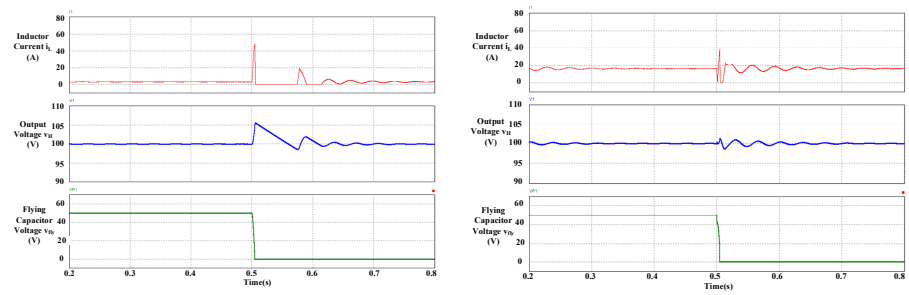

(**a**) (**b**)

Figure 17. The waveforms of S_3 short-circuit fault ($V_L < 0.5\ V_H$). (**a**) Light load 100 W; (**b**) heavy load 1000 W.

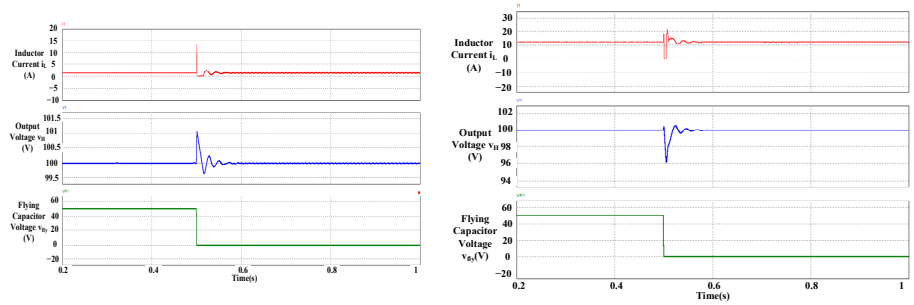

(**a**) (**b**)

Figure 18. The waveforms of S_3 short-circuit fault ($V_L > 0.5\ V_H$). (**a**) Light load 100 W; (**b**) heavy load 1000 W.

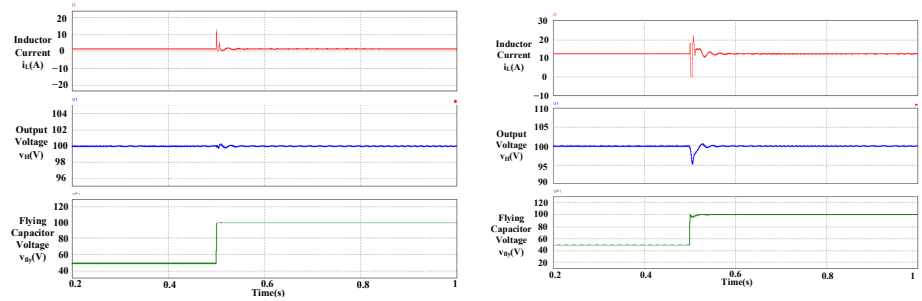

(**a**) (**b**)

Figure 19. The waveforms of S_4 short-circuit fault ($V_L > 0.5\ V_H$). (**a**) Light load 100 W; (**b**) heavy load 1000 W.

The simulation results when the input voltage is higher than half of the output voltage are shown in Figures 18 and 19. The waveforms when a short-circuit fault occurs in S_3 under two different load conditions including a light load and a heavy load are shown in Figure 18a,b, and the waveforms when a short-circuit fault occurs in S_4 under two different load conditions are shown in Figure 19a,b. It can also be seen that the output voltage is uninterruptible when two types of faults occur. The spike and surge of the current and voltage are also in the normal range.

The prototype of the three-level flying capacitor DC/DC converter is built to verify the fault-tolerant strategy. The parameters of the prototype are shown in Table 2.

Table 2. The parameters of the prototype of flying capacitor DC/DC converter.

Item	Value
Input voltage	10 V
Output DC bus voltage	32 V
Input inductor	100 μH
Flying capacitor	20 μF
Output bus capacitor	470 μF

The waveform when the short-circuit fault of S3 occurs is shown in Figure 20a. CH1 is the output voltage of the converter. CH2 is the flying capacitor voltage. CH3 is the trigger signal. CH4 is the driver signal of the power switch S3. The waveform of the three-level mode before the fault occurs is shown in Figure 20b. The waveform during the fault is shown in Figure 20c. It can be seen that the output voltage is uninterruptible and the flying capacitor voltage is regulated from 16 V to 0. The waveform of the two-level mode after the fault occurs is shown in Figure 20d. The waveform when the short-circuit fault of S4 occurs is shown in Figure 21a. The waveform before an S4 fault is shown in Figure 21b. The waveform during the fault is shown in Figure 21c. It can be seen that the output voltage is uninterruptible and the flying capacitor voltage is regulated from 16 V to 32 V. After the S4 fault, the waveform is shown in Figure 21d.

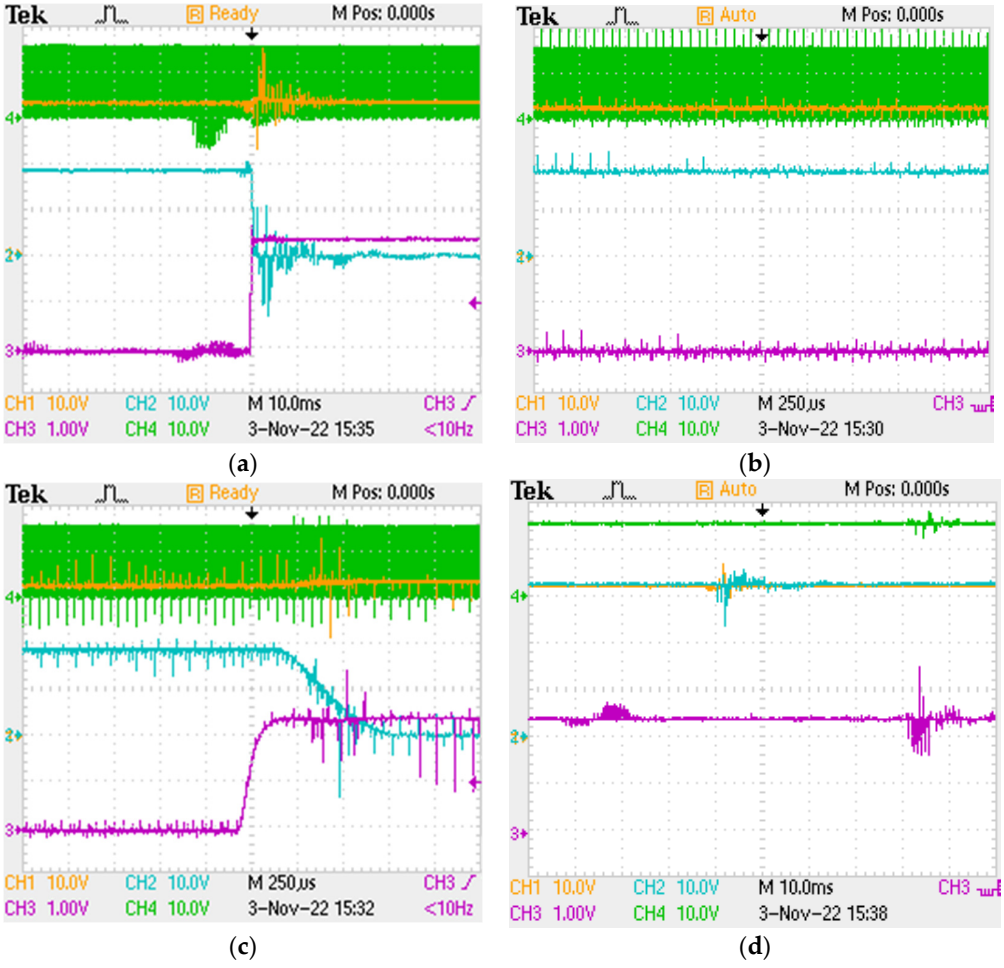

Figure 20. The experimental waveforms of S_3 short-circuit fault. (**a**) Overall stages; (**b**) the waveform of three-level mode before S_3 fault; (**c**) the waveform of S_3 short-circuit fault during fault; (**d**) the waveform of two-level mode after S_3 fault.

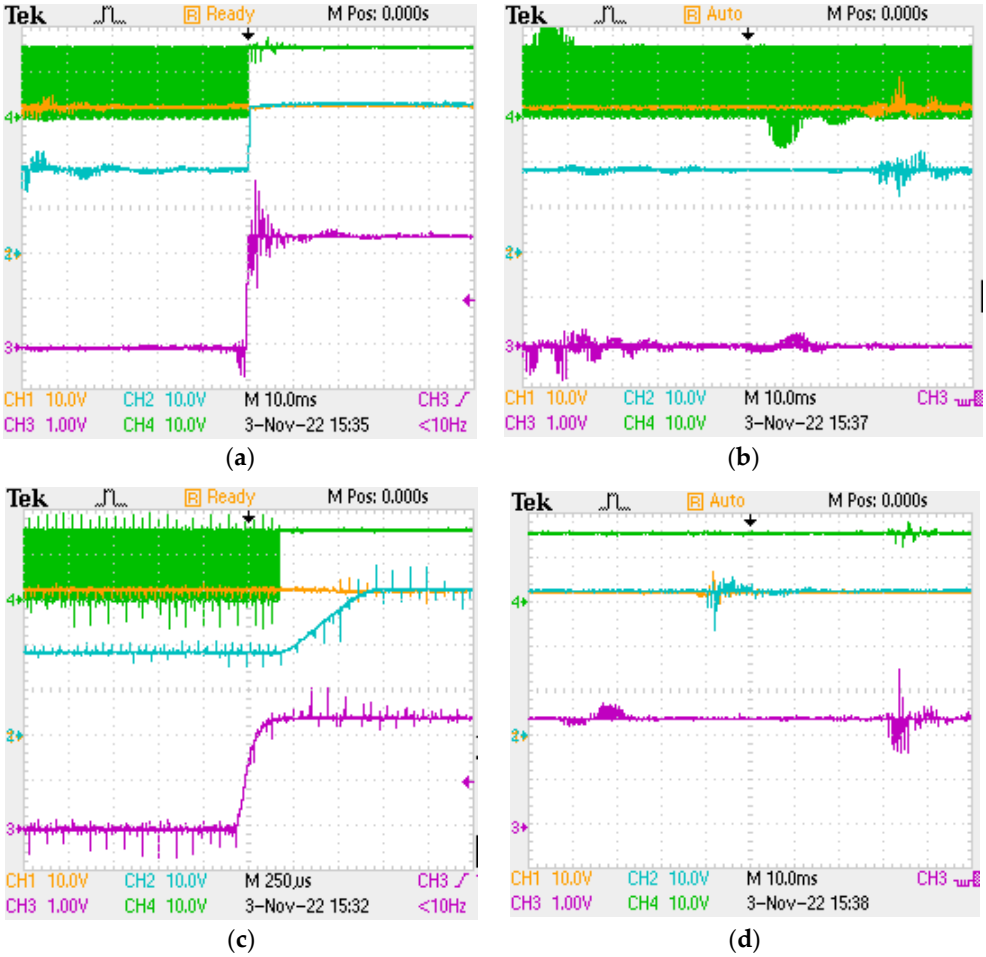

Figure 21. The experimental waveforms of S_4 short-circuit fault. (**a**) Overall stages; (**b**) the waveform of three-level mode before S_4 fault; (**c**) the waveform of S_4 short-circuit fault during fault; (**d**) the waveform of two-level mode after S_4 fault.

5. Conclusions

In order to improve the reliability of converters for the interface of the PV, battery, or other sources in spacecraft power systems for future high-voltage application, the fault-tolerant strategy of a three-level flying capacitor DC/DC converter is proposed in this paper. If a short-circuit fault occurs in the power devices, the converter can provide uninterruptible power for the load. It can turn from the three-level mode to the two-level mode, and during the mode transition, the voltage of the flying capacitor is regulated to the different target value based on the different fault locations. There is no extra hardware needed for this proposed strategy; the fault tolerance of the converter is only achieved by changing the software control strategy, and the reliability of the converter is improved with minimal cost. The stage analysis of the three-level converter is provided in detail. Different ratios between the input and output voltage and different fault locations are considered. Finally, a simulation model and prototype of the converter with the fault-tolerant strategy are built to verify the proposed strategy. The results show the fault tolerance operation of the converter is achieved after a short-circuit fault occurs.

Author Contributions: Conceptualization, H.L.; methodology, H.L., X.Z., Z.L. and Y.Z.; validation, H.L., Y.G. and L.Z. All authors have read and agreed to the published version of the manuscript.

Funding: This work is supported by the National Natural Science Foundation of China (52007007).

Institutional Review Board Statement: Not applicable.

Informed Consent Statement: Not applicable.

Data Availability Statement: Not applicable.

Conflicts of Interest: The authors declare no conflict of interest.

References

1. Zhang, X.; Li, H. Design of Software Defined Spacecraft Distributed Power Supply System. *Spacecr. Eng.* **2020**, *29*, 51–58.
2. Zhang, M.; Liu, Y.; Li, H.; Zhang, W.; Zhang, X.; Xia, N.; Zhu, L.; Mu, H.; Liu, Z. Design of 100kW Distributed Reconfigurable Electrical Power System for Spacecraft. *Spacecr. Eng.* **2021**, *30*, 86–94.
3. Bekemans, M.; Bronchart, F.; Scalais, T.; Franke, A. Configurable High Voltage Power Supply for Full Electric Propulsion Spacecraft. In Proceedings of the 2019 European Space Power Conference (ESPC 2019), Juan-les-Pins, France, 30 September–4 October 2019. [CrossRef]
4. Dusmez, S.; Hasanzadeh, A.; Khaligh, A. Comparative Analysis of Bidirectional Three-Level DC–DC Converter for Automotive Applications. *IEEE Trans. Ind. Electron.* **2014**, *62*, 3305–3315. [CrossRef]
5. Ruan, X.; Li, B.; Chen, Q.; Tan, S.-C.; Tse, C.K. Fundamental considerations of three-level DC–DC converters: Topologies, analyses, and control. *IEEE Trans. Circuits Syst. I Regul. Pap.* **2008**, *55*, 3733–3743. [CrossRef]
6. Kesarwani, K.; Stauth, J.T. Resonant and multi-mode operation of flying capacitor multi-level DC-DC converters. In Proceedings of the 2015 IEEE 16th Workshop on Control and Modeling for Power Electronics (COMPEL), Vancouver, BC, Canada, 12–15 July 2015; pp. 1–8.
7. Tesaki, K.; Ishida, Y.; Hagiwara, M. Control and Experimental Verification of a Bidirectional Non-isolated DC-DC Converter Based on Three-level Flying-Capacitor Converters. *IEEJ J. Ind. Appl.* **2021**, *10*, 114–123. [CrossRef]
8. Cuzner, R.M.; Bendre, A.R.; Faill, P.J.; Semenov, B. Implementation of a non-isolated three level DC/DC converter suitable for high power systems. In Proceedings of the 2007 IEEE Industry Applications Annual Meeting, New Orleans, LA, USA, 23–27 September 2007; pp. 2001–2008.
9. Choi, M.; Jeong, D.K. Design of High Step-Down Ratio Isolated Three-Level Half-Bridge DC–DC Converter With Balanced Voltage on Flying Capacitor. *IEEE Trans. Power Electron.* **2022**, *37*, 10213–10225. [CrossRef]
10. Zhong, Z.; Chen, Y.; Zhang, P.; Kang, Y. A cost-effective circuit for three-level flying-capacitor buck converter combining the soft-start, flying capacitor pre-charging and snubber functions. In Proceedings of the 2014 IEEE Energy Conversion Congress and Exposition (ECCE), Pittsburgh, PA, USA, 14–18 September 2014; pp. 3658–3663. [CrossRef]
11. Zhang, W.; Xu, D.; Enjeti, P.N.; Li, H.; Hawke, J.T.; Krishnamoorthy, H.S. Survey on Fault-Tolerant Techniques for Power Electronic Converters. *IEEE Trans. Power Electron.* **2014**, *29*, 6319–6331. [CrossRef]
12. Kumar, G.K.; Elangovan, D. Review on fault-diagnosis and fault-tolerance for DC–DC converters. *IET Power Electron.* **2020**, *13*, 1–13. [CrossRef]
13. Bento, F.; Cardoso, A.J.M. A comprehensive survey on fault diagnosis and fault tolerance of DC-DC converters. *Chin. J. Electr. Eng.* **2018**, *4*, 1–12. [CrossRef]
14. Gleissner, M.; Bakran, M.M. Design and control of fault-tolerant nonisolated multiphase multilevel DC–DC converters for automotive power systems. *IEEE Trans. Ind. Appl.* **2015**, *52*, 1785–1795.
15. Pazouki, E.; Sozer, Y.; De Abreu-Garcia, J.A. Fault Diagnosis and Fault-Tolerant Control Operation of Nonisolated DC–DC Converters. *IEEE Trans. Ind. Appl.* **2017**, *54*, 310–320. [CrossRef]
16. Wang, H.; Li, H.; Yan, C.; Xu, D. A Short-Circuit Fault-Tolerant Strategy for Three-Phase Four-Wire Flying Capacitor Three-Level Inverters. In Proceedings of the 2019 IEEE 10th International Symposium on Power Electronics for Distributed Generation Systems (PEDG), Xi'an, China, 3–6 June 2019; pp. 781–786. [CrossRef]
17. Xu, S.; Zhang, J.; Hang, J. Investigation of a Fault-Tolerant Three-Level T-Type Inverter System. *IEEE Trans. Ind. Appl.* **2017**, *53*, 4613–4623. [CrossRef]
18. Sheng, H.; Wang, F.; Tipton, C.W., IV. A fault detection and protection scheme for three-level DC–DC converters based on monitoring flying capacitor voltage. *IEEE Trans. Power Electron.* **2011**, *27*, 685–697. [CrossRef]
19. Choi, U.M.; Blaabjerg, F.; Lee, K.B. Study and Handling "Methods of Power IGBT Module Failures in Power Electronic Converter Systems. *IEEE Trans. Power Electron.* **2015**, *30*, 2517–2533. [CrossRef]
20. Soon, J.L.; Lu, D.D.C. Design of fuse–MOSFET pair for fault-tolerant DC/DC converters. *IEEE Trans. Power Electron.* **2016**, *31*, 6069–6074. [CrossRef]